

Uncertainty-Aware and Reliable Neural MIMO Receivers via Modular Bayesian Deep Learning

Tomer Raviv, Sangwoo Park, Osvaldo Simeone, and Nir Shlezinger

Abstract—Deep learning is envisioned to play a key role in the design of future wireless receivers. A popular approach to design learning-aided receivers combines deep neural networks (DNNs) with traditional model-based receiver algorithms, realizing hybrid model-based data-driven architectures. Such architectures typically include multiple modules, each carrying out a different functionality dictated by the model-based receiver workflow. Conventionally trained DNN-based modules are known to produce poorly calibrated, typically overconfident, decisions. Consequently, incorrect decisions may propagate through the architecture without any indication of their insufficient accuracy. To address this problem, we present a novel combination of Bayesian deep learning with hybrid model-based data-driven architectures for wireless receiver design. The proposed methodology, referred to as *modular Bayesian deep learning*, is designed to yield calibrated modules, which in turn improves both accuracy and calibration of the overall receiver. We specialize this approach for two fundamental tasks in multiple-input multiple-output (MIMO) receivers – equalization and decoding. In the presence of scarce data, the ability of modular Bayesian deep learning to produce reliable uncertainty measures is consistently shown to directly translate into improved performance of the overall MIMO receiver chain.

I. INTRODUCTION

Deep neural networks (DNNs) were shown to successfully learn complex tasks from data in domains such as computer vision and natural language processing. This dramatic success has led to a burgeoning interest in the design of DNN-aided communications receivers [2]–[6]. While traditional receiver algorithms are based on the mathematical modelling of signal transmission, propagation, and reception, DNN-based receivers learn their mapping from data without relying on such accurate modelling. Consequently, DNN-aided receivers can operate efficiently in scenarios where the channel model is unknown, highly complex, or difficult to optimize [7]. The incorporation of deep learning into receiver processing is thus often envisioned to be an important contributor to meeting the rapidly increasing demands of wireless systems in throughput, coverage, and robustness [8].

Parts of this work were presented at the 2023 IEEE International Conference on Communications (ICC) as the paper [1]. T. Raviv and N. Shlezinger are with the School of ECE, Ben-Gurion University of the Negev, Beer-Sheva, Israel (e-mail: tomerraviv95@gmail.com, nirshi@bgu.ac.il). S. Park and O. Simeone are with King’s Communication Learning & Information Processing (KCLIP) lab, Centre for Intelligent Information Processing Systems (CIIPS), at the Department of Engineering, King’s College London, U.K. (email: {sangwoo.park; osvaldo.simeone}@kcl.ac.uk). The work of T. Raviv and N. Shlezinger was partially supported by the Israeli Innovation Authority. The work of O. Simeone was partially supported by the European Union’s Horizon Europe project CENTRIC (101096379), by an Open Fellowship of the EPSRC (EP/W024101/1), by the EPSRC project (EP/X011852/1), and by Project REASON, a UK Government funded project under the Future Open Networks Research Challenge (FONRC) sponsored by the Department of Science Innovation and Technology (DSIT).

Despite their promise in facilitating physical layer communications, particularly in multiple-input multiple-output (MIMO) systems, the deployment of DNNs faces several challenges that may limit their direct applicability to wireless receivers. The dynamic nature of wireless channels combined with the limited computational and memory resources of wireless devices indicates that MIMO receiver processing is fundamentally distinct from conventional deep learning domains, such as computer vision and natural language processing [9], [10]. Specifically, the necessity for online training may arise due to the time-varying settings of wireless communications. Nonetheless, pilot data corresponding to new channels is usually scarce. DNNs trained using conventional deep learning mechanisms, i.e., via *frequentist learning*, are prone to overfitting in such settings [11]. Moreover, they are likely to yield poorly calibrated outputs [12], [13], e.g., produce wrong decisions with high confidence.

A candidate approach to design DNN-aided receivers that can be trained with limited data incorporates model-based receiver algorithms as a form of inductive bias into a *hybrid model-based data-driven architecture* [14]–[16]. One such model-based deep learning methodology is *deep unfolding* [17]. Deep unfolding converts an iterative optimizer into a discriminative machine learning system by introducing trainable parameters within each of a fixed number of iterations [16], [18]. Deep unfolded architectures treat each iteration as a trainable module, obtaining a modular and interpretable DNN architecture [19], with each module carrying out a specific functionality within a conventional receiver processing algorithm. Modularity is informed by domain knowledge, potentially enhancing the generalization capability of DNN-based receivers [20]–[25].

Hybrid model-based data-driven methods require less data to reliably train compared to black box architectures. Yet, the resulting system may be negatively affected by the inclusion of conventionally trained DNN-based modules, i.e., DNNs trained via frequentist learning [13]. This follows from the frequent overconfident decisions that are often produced by such conventional DNNs, particularly when learning from limited data sets. Such poorly calibrated DNN-based modules may propagate inaccurate predictions through the architecture without any indication of their insufficient accuracy.

The machine learning framework of *Bayesian learning* accommodates learning techniques with improved calibration compared with frequentist learning [13], [26]–[28]. In Bayesian deep learning, the parameters of a DNN are treated as random variables. Doing so provides means to quantify the *epistemic* uncertainty, which arises due to lack of training data. Bayesian deep learning was shown to improve the reliability of DNNs in wireless communication systems [29],

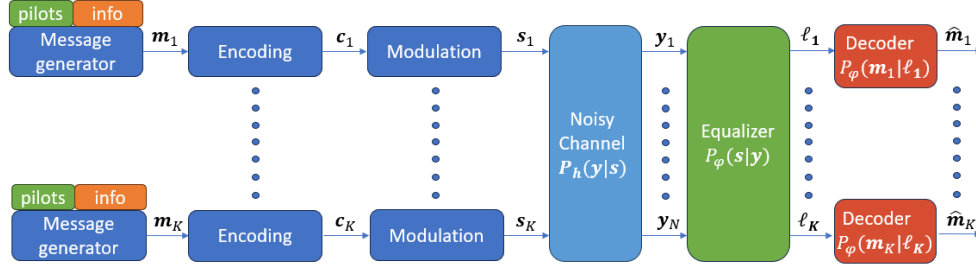


Fig. 1: The communication system studied in this paper.

[30]. Nonetheless, these existing studies adopt *black-box* DNN architectures. Thus, the existing approaches do not leverage the modularity of model-based data-driven receivers, and do not account for the ability to assign interpretable meaning to intermediate features exchanged in model-based deep learning architectures.

In this work we present a novel methodology, referred to as *modular Bayesian deep learning*, that combines Bayesian learning with hybrid model-based data-driven architectures for DNN-aided receivers. The proposed approach calibrates the internal DNN-based modules, rather than merely calibrating the overall system output. This has the advantage of yielding well-calibrated soft outputs that can benefit downstream tasks, as we empirically demonstrate.

Our main contributions are summarized as follows.

- **Modular Bayesian deep learning:** We introduce a modular Bayesian deep learning framework that integrates Bayesian learning with model-based deep learning. Accounting for the modular architecture of hybrid model-based data-driven receivers, Bayesian learning is applied on a per-module basis, enhancing the calibration of soft estimates exchanged between internal DNN modules. The training procedure is based on dedicated *sequential Bayesian learning* operation, which boosts calibration of internal modules while encouraging subsequent modules to exploit these calibrated features.
- **Modular Bayesian deep MIMO receivers:** We specialize the proposed methodology to MIMO receivers. To this end, we adopt two established DNN-aided architectures – the DeepSIC MIMO equalizer of [21] and the deep unfolded weighted belief propagation (WBP) soft decoder of [31] – and derive their design as modular Bayesian deep learning systems.
- **Extensive experimentation:** We evaluate the advantages of modular Bayesian learning for deep MIMO receivers based on DeepSIC and WBP. Our evaluation first considers equalization and decoding separately, followed by an evaluation of the overall receiver chain composed of the cascade of equalization and decoding. The proposed Bayesian modular approach is systematically shown to outperform conventional frequentist learning, as well as traditional Bayesian black-box learning, while being reliable and interpretable.

The remainder of this paper is organized as follows: Section II formulates the considered MIMO system model, and re-

views some necessary preliminaries on Bayesian learning and model-based deep receivers. Section III presents the proposed methodology of modular Bayesian learning, and specializes it for MIMO equalization using DeepSIC and for decoding using the WBP. Our extensive numerical experiments are reported in Section IV, while Section V provides concluding remarks.

Throughout the paper, we use boldface letters for multivariate quantities, e.g., \mathbf{x} is a vector; calligraphic letters, such as \mathcal{X} for sets, with $|\mathcal{X}|$ being the cardinality of \mathcal{X} ; and \mathcal{R} for the set of real numbers. The notation $(\cdot)^T$ stands for the transpose operation.

II. SYSTEM MODEL AND PRELIMINARIES

In this section, we describe the MIMO communication system under study in Subsection II-A, and review the conventional frequentist learning of MIMO receivers in Subsection II-B. Then, we briefly present basics of model-based learning for deep receivers in Subsection II-C, and review our main running examples of DeepSIC [21] and WBP [31].

A. System Model

We consider an uplink MIMO digital communication system with K single-antenna users. The users transmit encoded messages, independently of each other, to a base station equipped with N antennas. Each user of index k uses a linear block error-correction code to encode a length m binary message $\mathbf{m}_k \in \{0, 1\}^m$. Encoding is carried out by multiplication with a generator matrix \mathbf{G} , resulting in a length $C \geq m$ codeword given by $\mathbf{c}_k = \mathbf{G}^T \mathbf{m}_k \in \{0, 1\}^C$. The same codebook is employed for all users. The messages are modulated, such that each symbol $s_k[i]$ at the i th time index is a member of the set of constellation points \mathcal{S} . The transmitted symbols vector form the $K \times 1$ vector $\mathbf{s}[i] = [s_1[i] \dots s_K[i]] \in \mathcal{S}^K$.

We adopt a block-fading model, i.e., the channel remains constant within a block of duration dictated by the coherence time of the channel. A single block of duration T^{tran} is generally divided into two parts: the pilot part, composed of T^{pilot} pilots, and the message part of $T^{\text{info}} = T^{\text{tran}} - T^{\text{pilot}}$ information symbols. The corresponding indices for transmitted pilot symbols and information symbols are written as $\mathcal{T}^{\text{pilot}} = \{1, \dots, T^{\text{pilot}}\}$, and $\mathcal{T}^{\text{info}} = \{T^{\text{pilot}} + 1, \dots, T^{\text{tran}}\}$, respectively.

To accommodate complex and non-linear channel models, we represent the channel input-output relationship by a generic

conditional distribution. Accordingly, the corresponding received signal vector $\mathbf{y}[i] \in \mathcal{R}^N$ is determined as

$$\mathbf{y}[i] \sim P_{\mathbf{h}}(\mathbf{y}[i]|\mathbf{s}[i]), \quad (1)$$

which is subject to the unknown conditional distribution $P_{\mathbf{h}}(\cdot|\cdot)$ that depends on the current channel parameters \mathbf{h} .

The received channel outputs in (1) are processed by the receiver, whose goal is to recover correctly each message. This estimate of the k th user message is denoted by $\hat{\mathbf{m}}_k$. This mapping can be generally divided into two different tasks: (i) equalization and (ii) decoding. Equalization maps the received signal $\mathbf{y}[i]$ as an input into a vector of soft symbols estimates for each user, denoted $\hat{\mathbf{P}}_1[i], \dots, \hat{\mathbf{P}}_K[i]$. Decoding is done for each user separately, obtaining an estimation $\hat{\mathbf{m}}_k$ of the transmitted message from the soft probability vectors $\{\hat{\mathbf{P}}_k[i]\}_i$ corresponding to the codeword. The latter often involves first obtaining a soft estimate for each bit in the message, where we use $\hat{L}_k[v]$ to denote the estimated probability that the v th bit in the k th message is one. The entire communication chain is illustrated in Fig. 1.

B. Frequentist Deep Receivers

Deep receivers employ DNNs to map the block of channel output into the transmitted message, i.e., as part of the equalization and/or decoding operations. In conventional *frequentist* learning, optimization of the parameter vector φ dictating the receiver mappings is typically done by minimizing the cross-entropy loss using a labelled pair of inputs and outputs [3], i.e.,

$$\varphi^{\text{freq}} = \arg \min_{\varphi} \mathcal{L}_{\text{CE}}(\varphi). \quad (2)$$

For example, to optimize an equalizer (formulated here for a single user case for brevity), one employs $\mathcal{T}^{\text{pilot}}$ pilot symbols and their corresponding observed channel outputs to compute

$$\mathcal{L}_{\text{CE}}(\varphi) = -\frac{1}{|\mathcal{T}^{\text{pilot}}|} \sum_{i \in \mathcal{T}^{\text{pilot}}} \log P_{\varphi}(\mathbf{s}[i]|\mathbf{y}[i]). \quad (3)$$

In (3), $P_{\varphi}(\mathbf{s}[i]|\mathbf{y}[i])$ is the soft estimate associated with the symbol $\mathbf{s}[i]$ computed from $\mathbf{y}[i]$ with a DNN-aided equalizer with parameters φ . When such an equalizer is used, the stacking of $\{P_{\varphi}(\mathbf{s}[i]|\mathbf{y}[i])\}_{\mathbf{s} \in \mathcal{S}}$ forms the soft estimate $\hat{\mathbf{P}}[i]$.

Calibration is based on the reliability of its soft estimates. In particular, a prediction model $P_{\varphi}(\mathbf{s}[i]|\mathbf{y}[i])$ as in the above DNN-aided equalizer example is *perfectly calibrated* if the conditional distribution of the transmitted symbols given the predictor's output satisfies the equality [12]

$$P(\mathbf{s}[i] = \hat{\mathbf{s}}[i] | P_{\varphi}(\hat{\mathbf{s}}[i]|\mathbf{y}[i]) = \pi) = \pi \text{ for all } \pi \in [0, 1]. \quad (4)$$

When (4) holds, then the soft outputs of the prediction model coincide with the true underlying conditional distribution.

C. Hybrid Model-Based Data-Driven Architectures

As mentioned in Section I, two representative examples of hybrid model-based data-driven architectures employed by deep receivers are: (i) the DeepSIC equalizer of [21]; and (ii) the unfolded WBP introduced in [31], [32] for channel

Algorithm 1: DeepSIC Inference

Input: Channel output $\mathbf{y}[i]$; Parameter vector φ^{SIC} .

Output: Soft estimations for all users $\{\hat{\mathbf{P}}_k[i]\}_{k=1}^K$.

1 DeepSIC Inference

```

2   Generate an initial guess  $\{\hat{\mathbf{P}}^{(k,0)}\}_{k=1}^K$ .
3   for  $q \in \{1, \dots, Q\}$  do
4       for  $k \in \{1, \dots, K\}$  do
5           Calculate  $\hat{\mathbf{P}}^{(k,q)}$  by (5).
6   return  $\{\hat{\mathbf{P}}_k[i] = \hat{\mathbf{P}}^{(k,Q)}\}_{k=1}^K$ 
```

decoding. As these architectures are employed as our main running examples in the sequel, we next briefly recall their formulation.

1) *DeepSIC*: The DeepSIC architecture proposed in [21] is a modular model-based DNN-aided MIMO demodulator, based on the classic soft interference cancellation (SIC) algorithm [33]. SIC operates in Q iterations. This equalization algorithm refines an estimate of the conditional probability mass function for the constellation points in \mathcal{S} denoted by $\hat{\mathbf{P}}^{(k,q)}$, for each symbol transmitted by a user of index k , throughout the iterations $q = 1, \dots, Q$. The estimate is generated for every user $k \in \{1, \dots, K\}$ and every iteration $q \in \{1, \dots, Q\}$ by using the soft estimates $\{\hat{\mathbf{P}}^{(l,q-1)}\}_{l \neq k}$ of the interfering symbols $\{\mathbf{s}_l[i]\}_{l \neq k}$ obtained in the previous iteration $q - 1$ as well as the channel output $\mathbf{y}[i]$. This procedure is illustrated in Fig. 2(a).

In DeepSIC, interference cancellation and soft detection steps are implemented with DNNs. Specifically, the soft estimate of the symbol transmitted by k th user in the q th iteration is calculated by a DNN-based classifying module with parameter vector $\varphi^{(k,q)}$. Accordingly, the $|\mathcal{S}| \times 1$ probability mass function vector for user k at iteration q under time index i can be obtained as

$$\hat{\mathbf{P}}^{(k,q)} = \left\{ P_{\varphi^{(k,q)}}(\mathbf{s}|\mathbf{y}[i], \{\hat{\mathbf{P}}^{(l,q-1)}[i]\}_{l \neq k}) \right\}_{\mathbf{s} \in \mathcal{S}}, \quad (5)$$

where DeepSIC is parameterized by the set of model parameter vectors $\varphi^{\text{SIC}} = \{\{\varphi^{(k,q)}\}_{k=1}^K\}_{q=1}^Q$. The entire DeepSIC architecture is illustrated in Fig. 2(b) and its inference procedure is summarized in Algorithm 1.

In the original formulation in [21], DeepSIC is trained in a frequentist manner, i.e., by minimizing the cross-entropy loss (3). By treating each user $k = 1, \dots, K$ equally, the resulting loss is given by

$$\mathcal{L}_{\text{CE}}^{\text{SIC}}(\varphi) = \sum_{k=1}^K \mathcal{L}_{\text{CE}}^{\text{MSIC}}(\varphi^{(k,Q)}), \quad (6)$$

where the user-wise cross-entropy is evaluated over the pilot set $\mathcal{T}^{\text{pilot}}$ as

$$\begin{aligned} \mathcal{L}_{\text{CE}}^{\text{MSIC}}(\varphi^{(k,q)}) &= -\frac{1}{|\mathcal{T}^{\text{pilot}}|} \\ &\times \sum_{i \in \mathcal{T}^{\text{pilot}}} \log P_{\varphi^{(k,q)}}(\mathbf{s}_k[i]|\mathbf{y}[i], \{\hat{\mathbf{P}}^{(l,q-1)}[i]\}_{l \neq k}). \end{aligned} \quad (7)$$

In [21], the soft estimates for each user of index k were obtained via the final soft output, i.e., $\hat{\mathbf{P}}_k[i]$ is obtained as

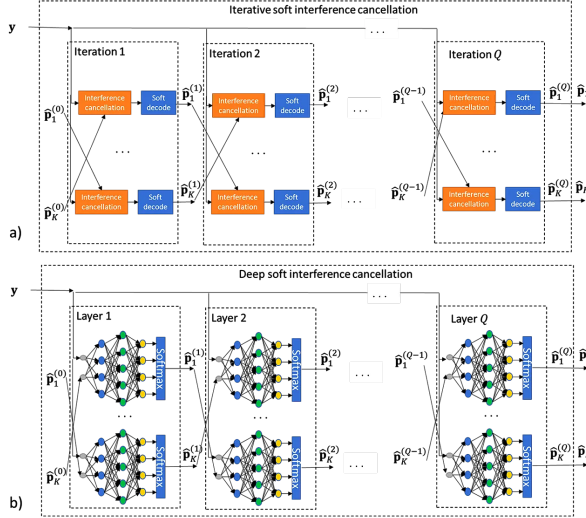


Fig. 2: (a) Iterative SIC; and (b) DeepSIC [21]. In this paper, we introduce modular Bayesian learning, which calibrates the internal modules of the DeepSIC architecture with the double goal of improving end-to-end accuracy and of producing well-calibrated soft outputs for the benefit of downstream tasks.

$\hat{P}^{(k,Q)}$. It was shown in [21] that under such setting, DeepSIC can outperform frequentist black-box deep receivers under limited pilots scenarios. However, its calibration performance is not discussed.

2) *Weighted Belief Propagation*: Belief propagation (BP) [34] is an efficient algorithm for calculating the marginal probabilities of a set of random variables whose relationship can be represented as a graph. A graphical representation used in channel coding is the Tanner graph of linear error-correcting codes [35]. A Tanner graph is a bipartite graph with two types of nodes: variable nodes and check nodes. The variable nodes correspond to bits of the encoded message, and the check nodes represent constraints that the message must satisfy.

In the presence of loops in the graph, BP is generally suboptimal. Its performance can be improved by weighting the messages via a learnable variant of the standard BP, called WBP [31], [32]. In WBP, the messages passed between nodes in the graphical model are weighted based on the relative soft-information they represent. These weights are learned from data by unfolding the message passing iterations of BP into a machine learning architecture. In particular, the message passing algorithm operates by iteratively passing messages over edges from variables nodes to check nodes and vice versa.

As the decoder is applied to each user separately, we omit the user index k in the following. To formulate the decoder, let the WBP message from variable node v to check node h at iteration q be denoted by $M_{v \rightarrow h}^{(q)}$, and from check node h to variable node v by $M_{h \rightarrow v}^{(q)}$. The messages are initialized $M_{v \rightarrow h}^{(q)} = M_{h \rightarrow v}^{(q)} = 0$ for all $(v, h) \in \mathcal{H}$, where \mathcal{H} denotes all valid variable-check connections. For instance, validity is determined for linear block codes by the element in the v th row and h th column in the parity check matrix. The input log likelihood ratio (LLR) values to the decoder are initialized from the outputs of the detection phase.

Algorithm 2: WBP Inference

Input: LLR values ℓ ; Parameter vector φ^{WBP} .

Output: Soft estimations for message bits $\hat{\mathbf{L}}$.

```

1 WBP Inference
2   Initialize  $M_{v \rightarrow h}^{(0)} = M_{h \rightarrow v}^{(0)} = 0$ .
3   for  $q \in \{1, \dots, Q\}$  do
4     for  $(v, h) \in \mathcal{H}$  do
5       Update  $M_{v \rightarrow h}^{(q)}$  by (8).
6     for  $(v, h) \in \mathcal{H}$  do
7       Update  $M_{h \rightarrow v}^{(q)}$  by (9).
8   Calculate  $\hat{\mathbf{L}}$  by (10) with  $q = Q$ .
9   return  $\hat{\mathbf{L}}$ 

```

To this end, one first finds the soft estimate $\tilde{c} \in \mathcal{R}^C$ of the codeword c . Given the i th soft symbol probability $\hat{P}[i]$, the soft estimate \tilde{c} can be found by translating $\hat{P}[i]$ to $r = \log_2 |\mathcal{S}|$ soft bits probabilities $\{\tilde{c}[i \cdot r], \dots, \tilde{c}[i \cdot r + r - 1]\}$ with $\tilde{c}[v] = P(c[v] = 1 | \hat{P}[i])$ for $v = i \cdot r, \dots, i \cdot r + r - 1$. Then the LLRs are computed by

$$\ell[v] = \log \frac{\tilde{c}[v]}{1 - \tilde{c}[v]},$$

and we use the vector ℓ to denote the stacking of $\ell[v]$ for all bit indices v corresponding to a given codeword.

After initialization, the iterative algorithm begins. Variable-to-check messages are updated according to the rule. i.e.,

$$M_{v \rightarrow h}^{(q)} = \tanh \left(\frac{1}{2} (\ell[v] + \sum_{\substack{(v, h') \in \mathcal{H} \\ h' \neq h}} \mathbf{W}_{h' \rightarrow v}^{(q)} M_{h' \rightarrow v}^{(q-1)}) \right), \quad (8)$$

with the parameters $\varphi^{(q)} = \{\mathbf{W}^{(q)}\}$, where $\mathbf{W}^{(q)}$ is a weights' matrix. The check-to-variable messages are updated by a non-weighted rule

$$M_{h \rightarrow v}^{(q)} = 2 \operatorname{arctanh} \left(\prod_{\substack{(v', h) \in \mathcal{H} \\ v' \neq v}} M_{v' \rightarrow h}^{(q)} \right). \quad (9)$$

The bit-wise probabilities are obtained from the messages via

$$\hat{L}^{(q)}[v] = \tanh \left(\frac{1}{2} (\ell[v] + \sum_{(v, h') \in \mathcal{H}} \mathbf{W}_{h' \rightarrow v}^{(q)} M_{h' \rightarrow v}^{(q-1)}) \right) \quad (10)$$

The update rules are performed on every combination of v, h for Q iterations. Finally, the codeword is estimated as the hard-decision on the probability vector $\hat{\mathbf{L}}$, which is the stacking of the bit-wise probabilities $\hat{L}^{(Q)}[v]$ for every v in the codeword. The entire inference procedure for a given WBP parameterization $\varphi^{\text{WBP}} = \{\varphi^{(q)}\}_{q=1}^Q$ is summarized in Algorithm 2.

The parameters of WBP, φ^{WBP} , are learned from data. Specifically, the decoder is trained to minimize the following cross-entropy multi-loss (3) over the pilots set $\mathcal{C}^{\text{pilot}} = \{1, \dots, r * T^{\text{pilot}}\}$

$$\mathcal{L}_{\text{CE}}^{\text{WBP}}(\varphi) = \sum_{q=1}^Q \mathcal{L}_{\text{CE}}^{\text{MWBP}}(\varphi^{(q)}), \quad (11)$$

Algorithm 3: Bayesian DeepSIC

Input: Channel output $\mathbf{y}[i]$; Distribution over entire architecture $p^b(\varphi^{\text{SIC}})$; Ensemble size J .

Output: Soft estimations for all users $\{\hat{\mathbf{P}}_k[i]\}_{k=1}^K$.

```

1 Bayesian Inference
2   for  $j \in \{1, \dots, J\}$  do
3     Generate  $\varphi_j^{\text{SIC}} \sim p^b(\varphi^{\text{SIC}})$ ;
4      $\{\hat{\mathbf{P}}_{k,j}[i]\}_{k=1}^K \leftarrow \text{DeepSIC}(\mathbf{y}[i], \varphi_j^{\text{SIC}})$ ;
5   return  $\{\hat{\mathbf{P}}_k[i] = \frac{1}{J} \sum_{j=1}^J \hat{\mathbf{P}}_{k,j}[i]\}_{k=1}^K$ 

```

with the cross-entropy loss at iteration q defined as

$$\mathcal{L}_{\text{CE}}^{\text{MWBP}}(\varphi^{(q)}) = -\frac{1}{|\mathcal{C}^{\text{pilot}}|} \sum_{v \in \mathcal{C}^{\text{pilot}}} \log P_{\varphi^{(q)}}(\mathbf{m}[v] | \ell[v], \{M_{h' \rightarrow v}^{(q-1)}\}). \quad (12)$$

In (12), $P_{\varphi^{(q)}}(\mathbf{m}[v] | \ell[v], \{M_{h' \rightarrow v}^{(q-1)}\})$ is the binary probability vector computed for the v th bit of the message, i.e., $\mathbf{m}[v]$.

III. MODULAR BAYESIAN DEEP LEARNING

Bayesian learning is known to improve the calibration of black-box DNNs models by preventing overfitting [29], [36]. In this section, we fuse Bayesian learning with hybrid model-based data-driven deep receivers. To this end, we first present the direct application of Bayesian learning to deep receivers in Subsection III-A, and illustrate the approach for DeepSIC and WBP in Subsection III-B. Then, we introduce the proposed modular Bayesian framework, and specialize it again to DeepSIC and WBP in Subsection III-C. We conclude with a discussion presented in Subsection III-D.

A. Bayesian Learning

Bayesian learning treats the parameter vector φ of a machine learning architecture as a *random vector*. This random vector obeys a distribution $p^b(\varphi)$ that accounts for the available data and for prior knowledge. Most commonly, the distribution is obtained by minimizing the *free energy loss*, also known as negative evidence lower bound (ELBO) [13], via

$$p^b(\varphi) = \arg \min_{p'} \left(\mathbb{E}_{\varphi \sim p'(\varphi)} [\mathcal{L}_{\text{CE}}(\varphi)] + \frac{1}{\beta} \text{KL}(p'(\varphi) || p^{\text{prior}}(\varphi)) \right). \quad (13)$$

The Kullback-Leibler (KL) divergence term in (13), given by

$$\text{KL}(p'(\varphi) || p(\varphi)) \triangleq \mathbb{E}_{p'(\varphi)} \left[\log \left(\frac{p'(\varphi)}{p(\varphi)} \right) \right],$$

regularizes the optimization of $p^b(\varphi)$ with a prior distribution $p^{\text{prior}}(\varphi)$. The hyperparameter $\beta > 0$, known as the inverse temperature parameter, balances the regularization impact [11], [13].

Algorithm 4: Bayesian WBP

Input: LLR values ℓ ; Distribution over entire architecture $p^b(\varphi^{\text{WBP}})$; Ensemble size J .

Output: Soft estimations for message bits $\hat{\mathbf{L}}$.

```

1 Bayesian Inference
2   for  $j \in \{1, \dots, J\}$  do
3     Generate  $\varphi_j^{\text{WBP}} \sim p^b(\varphi^{\text{WBP}})$ ;
4      $\hat{\mathbf{L}}_j \leftarrow \text{WBP}(\ell, \varphi_j^{\text{WBP}})$ ;
5   return  $\hat{\mathbf{L}} = \frac{1}{J} \sum_{j=1}^J \hat{\mathbf{L}}_j$ 

```

Once optimization based on (13) is carried out, Bayesian learning aims at having the output conditional distribution approximate the stochastic expectation

$$P_{p^b} = \mathbb{E}_{\varphi \sim p^b(\varphi)} [P_{\varphi}]. \quad (14)$$

The expected value in (14) is approximated by *ensemble* decision, namely, combining multiple predictions, with each decision based on a different realization of φ sampled from the optimized distribution $p^b(\varphi)$. Bayesian prediction (14) can account for the epistemic uncertainty residing in the optimal model parameters. This way, it can generally obtain a better calibration performance as compared to frequentist learning [29], [30].

B. Conventional Bayesian Learning for Deep Receivers

The conventional application of Bayesian learning includes obtaining the distribution over the set of model parameters vectors $p^b(\varphi)$. Afterwards, one can proceed to inference, where an ensembling over multiple realizations of parameters vectors, drawn from $p^b(\varphi)$, leads to more reliable estimate. Below, we specialize this case for our main running examples of deep receiver architectures: DeepSIC and WBP.

1) *DeepSIC*: The DeepSIC equalizer is formulated in Algorithm 1 for a deterministic (frequentist) parameter vector. When conventional Bayesian learning is employed, one obtains a distribution $p^b(\varphi^{\text{SIC}})$ over the set of model parameter vectors φ^{SIC} by minimizing the free energy loss (13). Using these distribution, the prediction for information symbols is computed as

$$P_{p^b}(\mathbf{s}_k[i] | \mathbf{y}[i]) = \mathbb{E}_{\varphi^{\text{SIC}} \sim p^b(\varphi^{\text{SIC}})} [P_{\varphi^{\text{SIC}}}(\mathbf{s}_k[i] | \mathbf{y}[i])], \quad (15)$$

for each data symbol at $i \in \mathcal{T}^{\text{info}}$, with soft prediction $\hat{\mathbf{P}}_k$ following (5). The resulting inference procedure is described in Algorithm 3.

While the final prediction $P_{\varphi^{\text{SIC}}}(\mathbf{s}_k[i] | \mathbf{y}[i])$ is obtained by ensembling the predictions of multiple parameter vectors $\varphi^{\text{SIC}} \sim p^b(\varphi^{\text{SIC}})$, the intermediate predictions made during SIC iterations, i.e., $\hat{\mathbf{P}}^{(k,q)}$ with $q < Q$, are not combined to approach a stochastic expectation. Thus, this form of Bayesian learning only encourages the outputs, i.e., the predictions at iteration Q , to be well calibrated, not accounting for the internal modular structure of the architecture. The soft estimates learned by the internal modules may still be overconfident, propagating inaccurate decisions to subsequent modules.

Algorithm 5: Modular Bayesian DeepSIC

Input: Channel output $\mathbf{y}[i]$; Distributions per module $\{p^{\text{mb}}(\varphi^{(k,q)})\}_{k=1}^K\}_{q=1}^Q$; Ensemble size J .

Output: Soft estimations for all users $\{\hat{P}_k[i]\}_{k=1}^K$.

```

1 Modular Bayesian Inference
2   Generate an initial guess  $\{\hat{P}^{(k,0)}\}_{k=1}^K$ .
3   for  $q \in \{1, \dots, Q\}$  do
4     for  $k \in \{1, \dots, K\}$  do
5       Bayesian Estimation Part
6       for  $j \in \{1, \dots, J\}$  do
7         Generate  $\varphi_j^{(k,q)} \sim p^{\text{mb}}(\varphi^{(k,q)})$ ;
8         Calculate  $\hat{P}_j^{(k,q)}$  by (5) using  $\varphi_j^{(k,q)}$ .
9          $\hat{P}^{(k,q)} = \frac{1}{J} \sum_{j=1}^J \hat{P}_j^{(k,q)}$ ;
10  return  $\{\hat{P}_k[i] = \hat{P}^{(k,Q)}\}_{k=1}^K$ 

```

2) *WBP*: Bayesian learning of WBP obtains a distribution $p^{\text{b}}(\varphi^{\text{WBP}})$ by the minimization of the free energy loss (13) using the pilots set $\mathcal{C}^{\text{pilot}}$. Once trained, the message bits are decoded via

$$P_{p^{\text{b}}}(\mathbf{m}[v]|\ell[v]) = \mathbb{E}_{\varphi^{\text{WBP}} \sim p^{\text{b}}(\varphi^{\text{WBP}})} [P_{\varphi^{\text{WBP}}}(\mathbf{m}[v]|\ell[v])], \quad (16)$$

for each data bit of index v in the information bits. The resulting inference procedure is described in Algorithm 4. As noted for DeepSIC, the resulting formulation only considers the soft estimate representation taken at the final iteration of index Q when approaching the stochastic expectation. Doing so fails to leverage the modular and interpretable operation of WBP to boost calibration of its internal message.

C. Modular Bayesian Learning for Deep Receivers

The conventional application of Bayesian deep learning is concerned with calibrating the final output of a DNN. As such, it does not exploit the modularity of model-based data-driven architectures, and particularly the ability to relate their internal features into probability measures. Here, we extend Bayesian deep learning to leverage this architecture of modular deep receivers. This is achieved by calibrating the intermediate blocks via Bayesian learning, combined with a dedicated *sequential Bayesian learning* procedure, as detailed next for DeepSIC and WBP.

1) *DeepSIC*: During training, we optimize the distribution $p^{\text{mb}}(\varphi^{(k,q)})$ over the parameter vector $\varphi^{(k,q)}$ of each block of index (k, q) , i.e., $\varphi^{(k,q)} \sim p^{\text{mb}}(\varphi^{(k,q)})$, individually. These distributions are obtained by minimizing the free energy loss on a per-module basis as

$$p^{\text{mb}}(\varphi^{(k,q)}) = \arg \min_{p'} \left(\mathbb{E}_{\varphi^{(k,q)} \sim p'(\varphi^{(k,q)})} [\mathcal{L}_{CE}^{\text{MSIC}}(\varphi^{(k,q)})] + \frac{1}{\beta} \text{KL}(p'(\varphi^{(k,q)}) || p^{\text{prior}}(\varphi^{(k,q)})) \right), \quad (17)$$

with the module-wise loss $\mathcal{L}_{CE}^{\text{MSIC}}(\varphi^{(k,q)})$ defined in (7).

The core difference in the formulation of the training objective in (17) as compared to (15) is that a single module

Algorithm 6: Modular Bayesian WBP

Input: LLR values ℓ ; Distributions per module $\{p^{\text{mb}}(\varphi^{(q)})\}_{q=1}^Q$; Ensemble size J .

Output: Soft estimations for message bits \hat{L} .

```

1 Modular Bayesian Inference
2   Initialize  $M_{v \rightarrow h}^{(q)} = M_{h \rightarrow v}^{(q)} = 0$ .
3   for  $q \in \{1, \dots, Q\}$  do
4     for  $(v, h) \in \mathcal{H}$  do
5       Bayesian Estimation Part
6       for  $j \in \{1, \dots, J\}$  do
7         Generate  $\varphi_j^{(q)} \sim p^{\text{mb}}(\varphi^{(q)})$ ;
8         Compute  $M_{v \rightarrow h, j}^{(q)}$  by (8) using  $\varphi_j^{(q)}$ ;
9          $M_{v \rightarrow h}^{(q)} = \frac{1}{J} \sum_{j=1}^J M_{v \rightarrow h, j}^{(q)}$ 
10    for  $(v, h) \in \mathcal{H}$  do
11      Update  $M_{h \rightarrow v}^{(q)}$  by (9).
12    Calculate  $\hat{L}$  by (10) with  $q = Q$ .
13  return  $\hat{L}$ 

```

is considered, rather than the entire model. Accordingly, the learning is done in a *sequential* fashion, where we first use (17) to train the modules corresponding to iteration $q = 1$, followed by training the modules for $q = 2$, and so on. This sequential Bayesian learning utilizes the calibrated soft estimates computed by using the data set at the q th iteration as inputs when training the modules at iteration $q + 1$. Doing so does not only improves the calibration of the intermediate modules, but also encourages them to learn with better calibrated soft estimates of the interfering symbols.

Once the modules corresponding to the q th iteration are trained, the soft estimate $\hat{P}^{(k,q)}[i]$ for the k th symbol at the q th iteration is computed by taking into account the uncertainty of the corresponding model parameter vector $\varphi^{(k,q)}$. The resulting expression is given by

$$\hat{P}^{(k,q)}[i] = \left\{ \mathbb{E}_{\varphi^{(k,q)} \sim p^{\text{mb}}(\varphi^{(k,q)})} \left[P_{\varphi^{(k,q)}}(s|\mathbf{y}[i], \{\hat{P}^{(l,q-1)}[i]\}_{l \neq k}) \right] \right\}_{s \in \mathcal{S}},$$

where again the stochastic expectation is approximated via ensembling.

Having computed a possibly different distribution for the weights of each intermediate module, prediction of the information symbols is computed by setting $\hat{P}_k[i] = \hat{P}^{(k,Q)}[i]$ for each data symbol at $i \in \mathcal{T}^{\text{info}}$. The resulting inference algorithm for the trained modular Bayesian DeepSIC is summarized in Algorithm 5.

2) *Weighted Belief Propagation*: Each internal messages of BP represents the belief on the value of a variable or check node. Modelling each message exchange iteration via a Bayesian deep architecture enables more reliable information exchange of such belief values. By doing so, one can prevent undesired quick convergence of the beliefs to polarized values from overconfident estimates, thus enhancing the reliability of the final estimate.

Carrying out WBP via modular Bayesian deep learning

requires learning a *per-module* basis distribution. Specifically, the per-module distribution is obtained by minimizing the free energy loss per module, i.e., each module q solves

$$p^{\text{mb}}(\varphi^{(q)}) = \arg \min_{p'} \left(\mathbb{E}_{\varphi^{(q)} \sim p'(\varphi^{(q)})} [\mathcal{L}_{CE}^{\text{MWBP}}(\varphi^{(q)})] + \frac{1}{\beta} \text{KL}(p'(\varphi^{(q)}) || p^{\text{prior}}(\varphi^{(q)})) \right),$$

where the module-wise loss $\mathcal{L}_{CE}^{\text{MWBP}}(\varphi^{(q)})$ is defined in (12). As detailed for modular Bayesian DeepSIC, training is carried out via sequential Bayesian learning, gradually learning the distribution of the parameters of each iteration, while using its calibrated outputs when training the parameters of the subsequent iteration.

In particular, each intermediate probability value is calculated based on realizations of parameters drawn from the obtained distribution, i.e.,

$$\hat{L}^{(q)}[v] = \mathbb{E}_{\varphi^{(q)} \sim p^{\text{mb}}(\varphi^{(q)})} \left[P_{\varphi^{(q)}}(\mathbf{m}[v] | \ell[v], \{M_{h' \rightarrow v}^{(q-1)}\}) \right],$$

where ensembling is used to approximate the expected value. The proposed inference procedure for modular Bayesian WBP is described in Algorithm 6.

D. Discussion

The core novelty of the algorithms formulated above lies in the introduction of the concept of modular Bayesian deep learning, specifically designed for hybrid model-based data-driven receivers, such as DeepSIC and WBP. Unlike conventional Bayesian approaches (see Algorithms 3 and 4) that focus solely on the output, our method applies Bayesian learning to each intermediate module, leading to increased reliability and performance at every stage of the network. Algorithms 5 and 6 illustrate the Bayesian estimation in intermediate layers.

Overall, this iterative gain in reliability propagates throughout the model, resulting in higher performance and reliability to classification tasks, such as detection and decoding. The consistent benefits of modular Bayesian learning are demonstrated through simulation studies in Section IV.

Our training algorithm relies on a sequential operation which gradually learns the distribution of each iteration-based module in a deep unfolded architecture, while using the calibrated predictions of preceding iterations. This learning approach has three core gains: (i) it facilitates individually assessing each module based on its probabilistic prediction; (ii) it enables the trainable parameters of subsequent iterations to adapt to already calibrated predictions of their preceding modules; and (iii) it facilitates an efficient usage of the available limited data obtained from pilots, as it reuses the entire data set for training each module. Specifically, when training each module individually, the data set is used to adapt a smaller number of parameters as compared to jointly training the entire architecture as in conventional end-to-end training. Nonetheless, this form of learning is expected to be more lengthy as compared to conventional end-to-end frequentist learning, due to its sequential operation combined with the

excessive computations of Bayesian learning (13). While one can possibly reduce training latency via, e.g., optimizing the learning algorithm [19], such extensions of our framework are left for future research.

IV. NUMERICAL EVALUATIONS

In this section we numerically quantify the benefits of the proposed modular Bayesian deep learning framework as compared to both frequentist learning and conventional Bayesian learning. We focus on uplink MIMO communications with DeepSIC detection and WBP decoding. We note that the relative performance of DeepSIC and WBP with frequentist learning in comparison to state-of-the-art receiver methods was studied in [21] and [31], respectively. Accordingly, here we focus on evaluating the performance gains of a receiver architecture based on DeepSIC and WBP *when modular Bayesian learning is adopted*, using as benchmarks frequentist learning and standard, non-modular, Bayesian learning. Specifically, after formulating the experimental setting and methods in Subsection IV-A, we study the effect of modular Bayesian learning for equalization and detection separately in Subsections IV-B-IV-C, respectively. Then, we assess the calibration of modular Bayesian equalization and its contribution to downstream soft decoding task in Subsection IV-D, after the full modular Bayesian receiver is evaluated in Subsection IV-E.

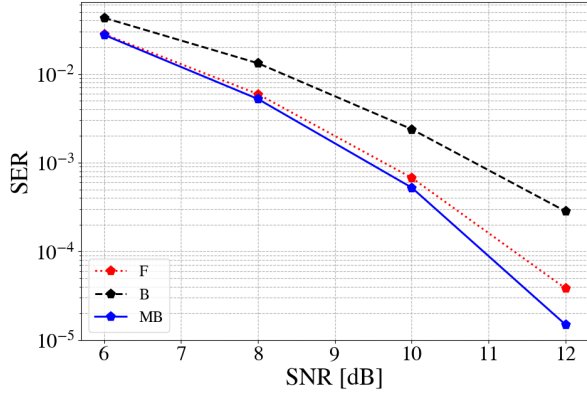
A. Architecture and Learning Methods

Architectures: The DNN-aided equalizer used in this study is based on the DeepSIC architecture [21], with DNN-modules comprised of three fully connected (FC) layers with a hidden layer size of 48 and ReLU activations unrolled over $Q = 3$ iterations. The decoder chosen is based on WBP [32], which is implemented over $Q = 5$ iterations with learnable parameters corresponding to messages of the variable-to-check layers (8). Choosing $Q = 5$ layers was empirically observed to reach satisfactory high performance gain over the vanilla BP [31], [32].

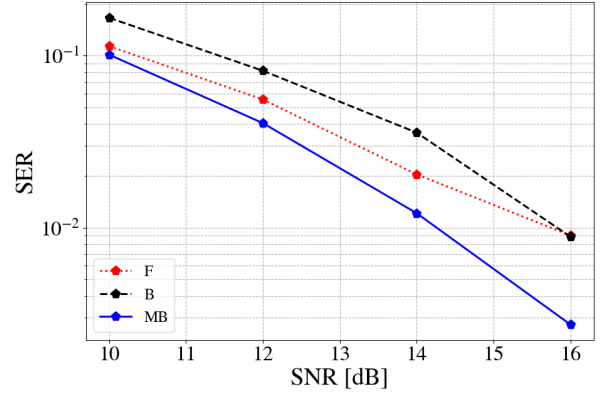
Learning Methods: For both detection and decoding, we compare the proposed modular Bayesian learning to both frequentist learning and Bayesian learning. Specifically, we employ the following three learning schemes:

- *Frequentist (F)*: This method, labelled as “F” in the figures, applies the conventional learning for training DeepSIC and WBP as detailed in Subsection II-B.
- *Bayesian (B)*: The conventional Bayesian receiver, referred to as “B”, carries out optimization of the distribution $p^b(\varphi)$ in an end-to-end fashion as described in Subsection III-B.
- *Modular Bayesian (MB)*: The proposed modular Bayesian learning scheme, introduced in Subsection III-C, that applies Bayesian learning separately to each module, and is labelled as “MB” in the figures.

For the Bayesian learning schemes “B” and “MB”, we adopt the Monte Carlo (MC) dropout scheme [36], [37], which parameterizes the distribution $p^b(\varphi)$ in terms of nominal



(a) QPSK constellation



(b) 8-PSK constellation

Fig. 3: Static linear synthetic channel: SER of DeepSIC as a function of the SNR for different training methods. At each block, training is done with 384 pilots, and the SER is computed on 14,976 information symbols from the QPSK or 8-PSK constellation. Results are averaged over 10 blocks per point.

model parameter vector and dropout probability vector. During Bayesian training, we set the inverse temperature parameter $\beta = 10^4$; and during Bayesian inference we set the ensemble size as $J = 5$ for DeepSIC and as $J = 3$ for WBP. For all of DeepSIC variations, optimization is done via Adam with 500 iterations and learning rate of $5 \cdot 10^{-3}$. For WBP, Adam with 500 iterations and learning rate of 10^{-3} was used. These values were set empirically to ensure convergence¹.

B. Detection Performance

We begin by evaluating the proposed modular Bayesian deep learning framework for symbol detection using the DeepSIC equalizer. We consider two types of different channels: (i) a static synthetic linear channel, and (ii) a time-varying channel obtained from the physically compliant COST simulator [38], both with additive Gaussian noise. The purpose of this study is to illustrate the benefits of employing the modular Bayesian approach to improve the detection performance in terms of symbol error rate (SER).

1) *Static Linear Synthetic Channels*: The considered input-output relationship of the memoryless Gaussian MIMO channel is given by

$$\mathbf{y}[i] = \mathbf{H}\mathbf{s}[i] + \mathbf{w}[i], \quad (18)$$

where \mathbf{H} is a fixed $N \times K$ channel matrix, and $\mathbf{w}[i]$ is a complex white Gaussian noise vector. The matrix \mathbf{H} models spatial exponential received power decay, and its entries are given by $(\mathbf{H})_{n,k} = e^{-|n-k|}$, for each $n \in \{1, \dots, N\}$ and $k \in \{1, \dots, K\}$. The pilots and the transmitted symbols are generated in a uniform i.i.d. manner over two different constellations, the first being the quadrature phase shift keying (QPSK) constellation, i.e., $\mathcal{S} = \{(\pm 1/\sqrt{2}, \pm 1/\sqrt{2})\}$, and the second being 8-ary phase shift keying (8-PSK) constellation, i.e., $\mathcal{S} = \{e^{j\frac{2\pi\ell}{8}} | \ell \in \{0, \dots, 7\}\}$. For both cases, the number of users and antennas are set as $K = N = 4$.

We evaluate the accuracy of hard detection in terms of SER, i.e., as the average $\frac{1}{K} \sum_k \mathbb{E}[\mathbb{1}(\hat{s}_k[i] \neq s_k[i])]$, with

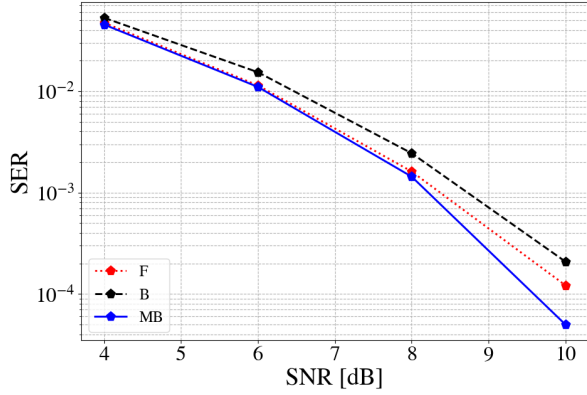
$\mathbb{1}(\cdot)$ being the indicator function, and where the expectation is estimated using the transmitted symbols and the noise in (18). Specifically, the block is composed of $T^{\text{pilot}} = 384$ pilot symbols, and $T^{\text{info}} = 14,976$ information symbols, for a total number of symbols $T^{\text{tran}} = 15,360$ in a single block for both constellations. The pilots amount to only 2.5% of the total block size.

The resulting SER performance versus signal-noise ratio (SNR) are reported in Fig. 3. The gains of the modular Bayesian DeepSIC (“MB”) are apparent. Specifically, “MB” consistently outperforms the frequentist DeepSIC (“F”) by up to 0.7 dB under QPSK in medium-to-high SNRs, and by up to 1.5 dB when the 8-PSK constellation is considered. The explanation for this performance gap lies in the severe data-deficit conditions. Due to limited data, the frequentist and the black-box Bayesian (“B”) methods are severely overfitted, particularly in the 8-PSK case. In particular, conventional Bayesian learning succeeds in calibrating the output of the receiver, but not of the intermediate blocks, increasing the reliability at the expense of the accuracy.

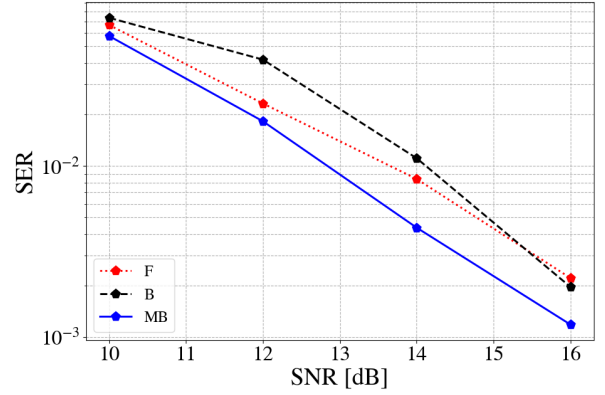
It is also noted that the gain of the proposed “MB” approach as compared to “F” and “B” becomes more pronounced with an increasing SNR level. To understand this behavior, it is useful to decompose the uncertainty that affects data-driven solutions into *aleatoric uncertainty* and *epistemic uncertainty*. Aleatoric uncertainty is the inherent uncertainty present in data, e.g., due to channel noise; while epistemic uncertainty is the uncertainty that arises from lack of training data. Since both the frequentist and Bayesian learning suffer equally from aleatoric uncertainty, the gain of Bayesian learning becomes highlighted with reduced aleatoric uncertainty, i.e., with an increased SNR (see, e.g., [13, Sec. 4.5.2] for a detailed discussion).

2) *Time-Varying Linear COST Channels*: Next, we evaluate the proposed model-based Bayesian scheme under the time-varying COST 2100 geometry-based stochastic channel model [38]. The simulated setting represents multiple users moving in an indoor setup while switching between different microcells. Succeeding on this scenario requires high adaptivity, since

¹The source code used in our experiments is available at <https://github.com/tomerraviv95/bayesian-learning-in-receivers-for-decoding>



(a) QPSK constellation



(b) 8-PSK constellation

Fig. 4: Time-varying COST channel: SER of DeepSIC as a function of the SNR for different training methods. At each block, training is done with 384 pilots, and the SER is computed on 14,976 information symbols from the QPSK or 8-PSK constellation. Results are averaged over 10 blocks per point.

there is considerable variability in the channels observed in different blocks. The employed channel model has the channel coefficients change in a block-wise manner. The instantaneous channel matrix is simulated using the wide-band indoor hall 5 GHz setting of COST 2100 with single-antenna elements, which creates $4 \times 4 = 16$ narrow-band channels when setting $K = N = 4$.

For the same hyperparameters as in Subsection IV-B1, in Fig. 4, we report the SER as a function of the SNR for both QPSK and 8-PSK after the transmission of 10 blocks. The main conclusion highlighted above, in the synthetic channel, is confirmed in this more realistic setting. It is systematically observed that modular Bayesian learning yields notable SER improvements, particularly for higher-order constellations, where overfitting is more pronounced.

C. Decoding Performance

We proceed to evaluating the contribution of modular Bayesian learning to channel decoding. To that end, prior to the symbols' transmission, the message is encoded via polar code (128,64) (as in the 5G standard). The WBP decoder is either trained using frequentist ("F"), Bayesian ("B"), or modular Bayesian ("MB") methods, and is applied following soft equalization using DeepSIC. We henceforth use the notation "X/Y" with $X, Y \in \{F, B, MB\}$ to indicate that the soft equalizer whose outputs are fed to WBP for decoding is DeepSIC trained using method "X", while WBP is trained using "Y". As our focus in this subsection is only on the decoder, we consider frequentist detection only. In all cases, we trained DeepSIC, and then trained the WBP decoder on the soft outputs obtained by the corresponding DeepSIC detector according to (11). This way, the decoder is optimized to make use of the detector's soft outputs.

To evaluate modular Bayesian learning of channel decoders, we consider a binary phase shift keying (BPSK) constellation. We use 1,536 pilot symbols, while the rest of the hyperparameters chosen as in Subsection IV-B1. For the considered setup, Fig 5 depicts the decoding bit error rate (BER) versus SNR.

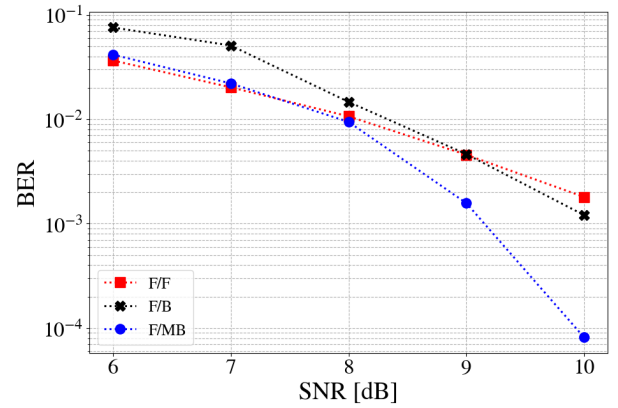


Fig. 5: Decoding performance: BER as a function of SNR for either a frequentist, a Bayesian or a modular Bayesian WBP decoder. DeepSIC is trained by the frequentist method.

Large gains to decoding are observed by employing the modular Bayesian method. This stands in contrast to the black-box Bayesian approach, which may degrade performance at high SNR values. This behavior is in line with a similar observation regarding DeepSIC trained in an end-to-end frequentist manner with a low number of training samples, as reported in [21, Fig. 10].

D. Calibration and Its Effect on Decoding Gain

As briefly mentioned in Subsection III-D, applying modular Bayesian learning in equalization can also benefit decoding performance for the two following reasons: (i) increased accuracy for hard detection, i.e., lower SER (as reported in Subsection IV-B); and (ii) increased calibration performance for soft detection which results in more reliable LLRs provided to the decoders. To evaluate the individual contribution of each of these factors, we next compute the expected calibration error (ECE) [39], which is conventionally used as a scalar measure of calibration performance (see also [12] for other

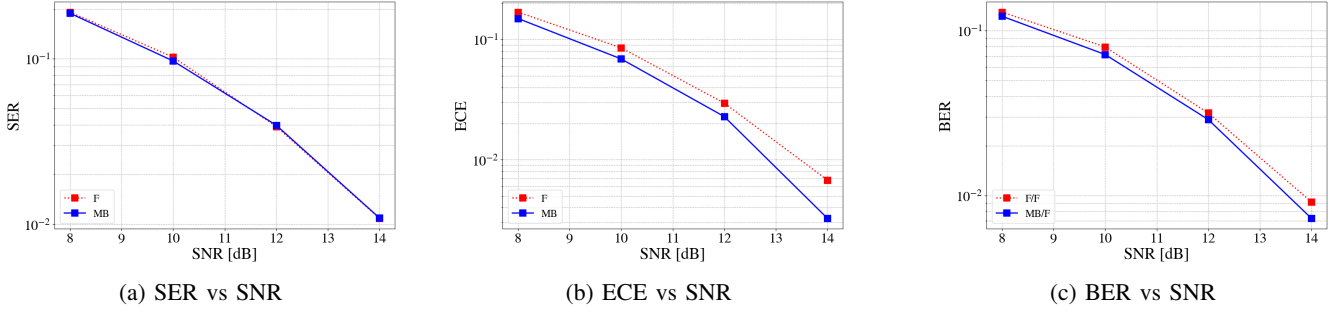


Fig. 6: Analysis of decoding gain: SER, ECE, and BER as a function of SNR for frequentist and modular Bayesian detector followed by a frequentist decoder.

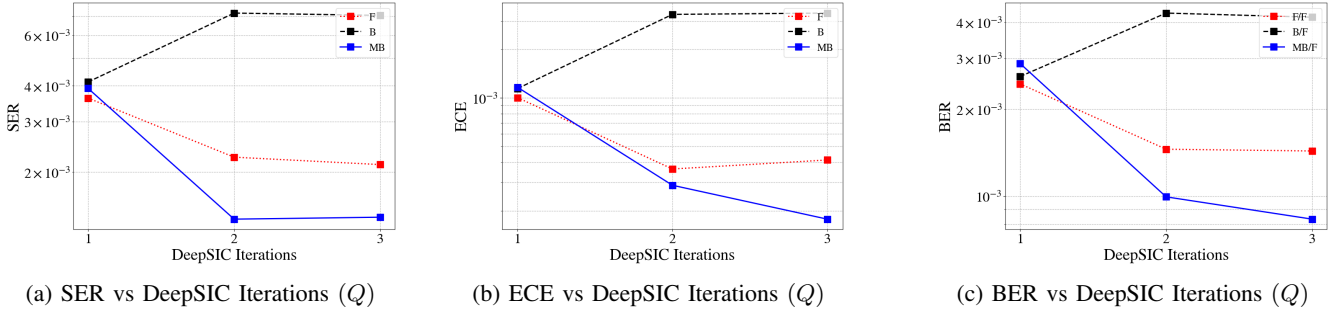


Fig. 7: Analysis of decoding gain: SER, ECE, and BER as a function of the number of iterations in DeepSIC for frequentist, Bayesian, and modular Bayesian detectors followed by a frequentist decoder.

calibration measures), and evaluate its contribution to soft decoding.

To formulate the ECE measure, let us partition the interval $[0, 1]$ of values for the *confidence level*, i.e., for the final soft output \hat{P}_k (obtained from either frequentist learning, Bayesian learning, or modular Bayesian learning), into R intervals $\{(0, 1/R], \dots, (R-1/R, 1]\}$. Define the r th bin as the collection of information-symbol indices that have the corresponding confidence values lying in the r th interval, i.e.,

$$\mathcal{T}_r = \{i \in \mathcal{T}^{\text{info}}, \forall k : P(\hat{s}_k[i] | \mathbf{y}_k[i]) \in (\frac{r-1}{R}, \frac{r}{R}]\}. \quad (19)$$

Accordingly, the *within-bin accuracy* and *within-bin confidence* are respectively computed for each m th bin as

$$\text{Acc}(\mathcal{T}_r) = \frac{1}{|\mathcal{T}_r|} \sum_{i \in \mathcal{T}_r, \forall k} \mathbb{1}(\hat{s}_k[i] = \mathbf{s}_k[i]), \quad (20)$$

$$\text{Conf}(\mathcal{T}_r) = \frac{1}{|\mathcal{T}_r|} \sum_{i \in \mathcal{T}_r, \forall k} P(\hat{s}_k[i] | \mathbf{y}_k[i]). \quad (21)$$

For a perfectly calibrated model as per (4), the within-bin accuracy $\text{Acc}(\mathcal{T}_r)$ must equal the within-bin confidence $\text{Conf}(\mathcal{T}_r)$ for every bin $r = 1, \dots, R$ given a sufficiently large set of information symbols $\mathcal{T}^{\text{info}}$. The ECE computes the average absolute difference between the within-bin accuracy and within-bin confidence, weighted by the number of samples that lie in each range, i.e.,

$$\text{ECE} = \sum_{r=1}^R \frac{|\mathcal{T}_r|}{\sum_{r'=1}^R |\mathcal{T}_{r'}|} \left(|\text{Acc}(\mathcal{T}_r) - \text{Conf}(\mathcal{T}_r)| \right). \quad (22)$$

The smaller the ECE is, the better calibrated the detector is. In the following analysis, we set the number of confidence bins

to $R = 10$

In Fig. 6, we study the impact of the learning method for the detector by plotting the SER, ECE, and BER for frequentist and modular Bayesian DeepSIC. Here, we implemented DeepSIC with a single iteration $Q = 1$, followed by a standard frequentist decoder. Note that in this case, modular Bayesian DeepSIC and Bayesian DeepSIC coincide. The advantage of Bayesian learning for the detector is seen to be exclusively in terms of ECE, since the SER is similar for frequentist and modular Bayesian DeepSIC across the considered range of SNRs. The improved calibration is observed to yield a decrease in the BER as the decoding module can benefit from the more reliable soft outputs of the Bayesian detector, as can be clearly observed in Figs. 6b-6c.

Next, we investigate how reliable information exchange between the modules within the detector affects the hard-decision performance. Towards this goal, in Fig. 7, we vary the modular structure of the DeepSIC detector by changing the number of iterations Q . We set the SNR to 15 dB, and measure the SER, ECE, and BER for $Q \in \{1, 2, 3\}$. With a higher number of iterations $Q > 1$, modular Bayesian DeepSIC is better able to exploit the modular structure, achieving both a lower SER and a lower ECE as compared to frequentist and Bayesian DeepSIC. Its improved reliability and SER are jointly translated at the output of the decoder into a lower BER, as demonstrated in Fig. 7.

E. Overall Receiver Evaluation

We conclude our numerical evaluation by assessing the contribution of adopting modular Bayesian both in detection and decoding. To that end, we compare the “F/F”, “F/MB”, “MB/F”

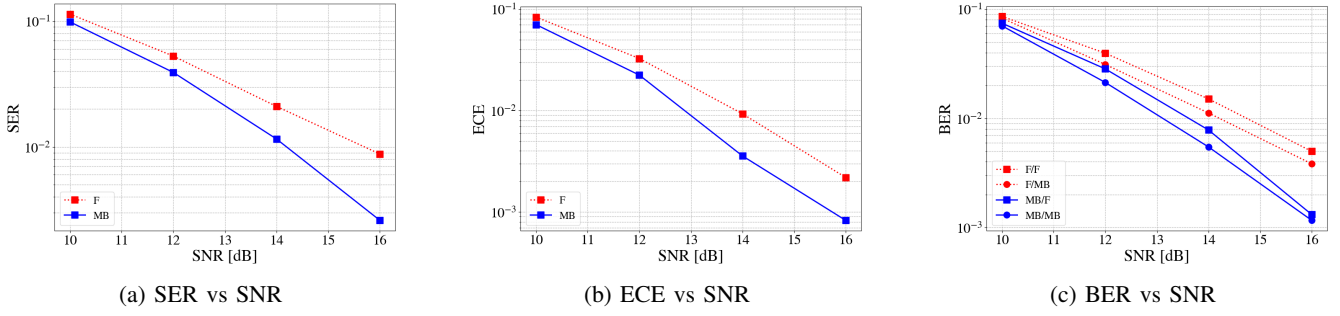


Fig. 8: Overall evaluation for the synthetic channel: SER, ECE and BER versus SNR for the combination of either a frequentist or modular Bayesian DeepSIC followed by either a frequentist or modular Bayesian WBP decoder.

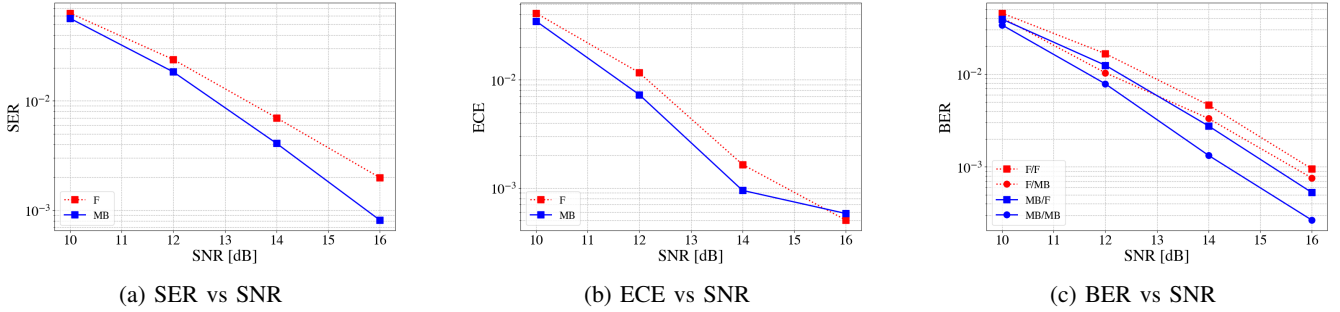


Fig. 9: Overall evaluation for the COST channel: SER, ECE and BER versus SNR for the combination of either a frequentist or modular Bayesian DeepSIC followed by either a frequentist or modular Bayesian WBP decoder.

and “MB/MB” methods for 8-PSK, with either the static synthetic channel from Subsection IV-B1 or the time-varying COST from Subsection IV-B2 using the same hyperparameters.

The performance achieved by the overall DNN-aided receiver for different training schemes, when applied in the channel of Subsection IV-B1, is reported in Fig. 8. In particular, Fig. 8a shows that the gain achievable by adopting our scheme is up to 1.5dB in SER. Due to this SER gain and the improved ECE as shown in Fig. 8b, the “MB/F” in Fig. 8c is shown to have similar gain in BER. Moreover, adopting modular Bayesian in both detection and decoding (“MB/MB”) is observed to have consistent gains that add up to 0.25dB.

Fig. 9 reports the results for the COST channel model. We note that Fig 9 further reinforces the superiority of our scheme, proving the gains of the “MB/MB” method over the “F/F” are also apparent over a more practical channel. Under this channel, the gains of adopting modular Bayesian decoding are higher, while the gains of modular Bayesian detection are slightly smaller, with both contributing up to 0.8dB each.

V. CONCLUSION

We have introduced modular Bayesian learning, a novel integration of Bayesian learning with hybrid model-based data-driven architectures, for wireless receiver design. The proposed approach harnesses the benefits of Bayesian learning in producing well-calibrated soft outputs for each internal module, hence resulting in performance improvement via reliable information exchange across the internal modules. We have shown that applying modular Bayesian learning to the

system with a cascade of modules, in which each module is composed of multiple internal modules, can yield a significant performance gain, e.g., BER gains of up to 1.6 dB.

Our proposed modular Bayesian learning, integrated with model-based deep learning, is designed for deep receivers. However, its underlying design principles are expected to be useful for a broad range of tasks where modular deep architectures are employed. These include, e.g., modular DNNs designed for dynamic systems [40], [41] and array signal processing tasks [42]. Moreover, our deviation focuses on improving reliability via Bayesian learning. However, Bayesian learning may not improve the reliability of the modules whenever its assumption has been made wrong, e.g., prior misspecification and/or likelihood misspecification [43]–[45]. This gives rise to a potential extension that replace Bayesian learning with robust Bayesian learning [29], possibly combined with conformal prediction [46]–[48]. These extensions are left for future work.

REFERENCES

- [1] T. Raviv, S. Park, O. Simeone, and N. Shlezinger, “Modular model-based Bayesian learning for uncertainty-aware and reliable deep MIMO receivers,” in *Proc. IEEE ICC*, 2023.
- [2] D. Gündüz, P. de Kerret, N. D. Sidiropoulos, D. Gesbert, C. R. Murthy, and M. van der Schaar, “Machine learning in the air,” *IEEE J. Sel. Areas Commun.*, vol. 37, no. 10, pp. 2184–2199, 2019.
- [3] O. Simeone, “A very brief introduction to machine learning with applications to communication systems,” *IEEE Trans. on Cogn. Commun. Netw.*, vol. 4, no. 4, pp. 648–664, 2018.
- [4] A. Balatsoukas-Stimming and C. Studer, “Deep unfolding for communications systems: A survey and some new directions,” *arXiv preprint arXiv:1906.05774*, 2019.

- [5] N. Farsad, N. Shlezinger, A. J. Goldsmith, and Y. C. Eldar, "Data-driven symbol detection via model-based machine learning," *arXiv preprint arXiv:2002.07806*, 2020.
- [6] Q. Mao, F. Hu, and Q. Hao, "Deep learning for intelligent wireless networks: A comprehensive survey," *IEEE Commun. Surveys Tuts.*, vol. 20, no. 4, pp. 2595–2621, 2018.
- [7] L. Dai, R. Jiao, F. Adachi, H. V. Poor, and L. Hanzo, "Deep learning for wireless communications: An emerging interdisciplinary paradigm," *IEEE Wireless Commun.*, vol. 27, no. 4, pp. 133–139, 2020.
- [8] W. Saad, M. Bennis, and M. Chen, "A vision of 6G wireless systems: Applications, trends, technologies, and open research problems," *IEEE Network*, vol. 34, no. 3, pp. 134–142, 2019.
- [9] T. Raviv, S. Park, O. Simeone, Y. C. Eldar, and N. Shlezinger, "Adaptive and flexible model-based AI for deep receivers in dynamic channels," *IEEE Wireless Commun.*, AI for deep access, 2023.
- [10] L. Chen, S. T. Jose, I. Nikoloska, S. Park, T. Chen, and O. Simeone, "Learning with limited samples: Meta-learning and applications to communication systems," *Foundations and Trends® in Signal Processing*, vol. 17, no. 2, pp. 79–208, 2023.
- [11] S. T. Jose and O. Simeone, "Free energy minimization: A unified framework for modelling, inference, learning, and optimization," *IEEE Signal Process. Mag.*, vol. 38, no. 2, pp. 120–125, 2021.
- [12] C. Guo, G. Pleiss, Y. Sun, and K. Q. Weinberger, "On calibration of modern neural networks," in *International Conference on Machine Learning*. PMLR, 2017, pp. 1321–1330.
- [13] O. Simeone, *Machine learning for engineers*. Cambridge University Press, 2022.
- [14] N. Shlezinger, J. Whang, Y. C. Eldar, and A. G. Dimakis, "Model-based deep learning," *Proc. IEEE*, vol. 111, no. 5, pp. 465–499, 2023.
- [15] N. Shlezinger, Y. C. Eldar, and S. P. Boyd, "Model-based deep learning: On the intersection of deep learning and optimization," *IEEE Access*, vol. 10, pp. 115 384–115 398, 2022.
- [16] N. Shlezinger and Y. C. Eldar, "Model-based deep learning," *Foundations and Trends® in Signal Processing*, vol. 17, no. 4, pp. 291–416, 2023.
- [17] V. Monga, Y. Li, and Y. C. Eldar, "Algorithm unrolling: Interpretable, efficient deep learning for signal and image processing," *IEEE Signal Process. Mag.*, vol. 38, no. 2, pp. 18–44, 2021.
- [18] N. Shlezinger and T. Routtenberg, "Discriminative and generative learning for the linear estimation of random signals [lecture notes]," *IEEE Signal Process. Mag.*, vol. 40, no. 6, pp. 75–82, 2023.
- [19] T. Raviv, S. Park, O. Simeone, Y. C. Eldar, and N. Shlezinger, "Online meta-learning for hybrid model-based deep receivers," *IEEE Trans. Wireless Commun.*, vol. 22, no. 10, pp. 6415–6431, 2023.
- [20] N. Shlezinger, N. Farsad, Y. C. Eldar, and A. J. Goldsmith, "Data-driven factor graphs for deep symbol detection," in *Proc. IEEE ISIT*, 2020, pp. 2682–2687.
- [21] N. Shlezinger, R. Fu, and Y. C. Eldar, "DeepSIC: Deep soft interference cancellation for multiuser MIMO detection," *IEEE Trans. Wireless Commun.*, vol. 20, no. 2, pp. 1349–1362, 2021.
- [22] N. Shlezinger, N. Farsad, Y. C. Eldar, and A. Goldsmith, "Viterbinet: A deep learning based Viterbi algorithm for symbol detection," *IEEE Trans. Wireless Commun.*, vol. 19, no. 5, pp. 3319–3331, 2020.
- [23] T. Raviv, N. Raviv, and Y. Be'ery, "Data-driven ensembles for deep and hard-decision hybrid decoding," in *Proc. IEEE ISIT*, 2020, pp. 321–326.
- [24] T. Van Luong, N. Shlezinger, C. Xu, T. M. Hoang, Y. C. Eldar, and L. Hanzo, "Deep learning based successive interference cancellation for the non-orthogonal downlink," *IEEE Trans. Veh. Technol.*, vol. 71, no. 11, pp. 11 876–11 888, 2022.
- [25] P. Jiang, T. Wang, B. Han, X. Gao, J. Zhang, C.-K. Wen, S. Jin, and G. Y. Li, "AI-aided online adaptive OFDM receiver: Design and experimental results," *IEEE Trans. Wireless Commun.*, vol. 20, no. 11, pp. 7655–7668, 2021.
- [26] L. V. Jospin, H. Laga, F. Boussaid, W. Buntine, and M. Bennamoun, "Hands-on Bayesian neural networks—a tutorial for deep learning users," *IEEE Comput. Intell. Mag.*, vol. 17, no. 2, pp. 29–48, 2022.
- [27] D. T. Chang, "Bayesian neural networks: Essentials," *arXiv preprint arXiv:2106.13594*, 2021.
- [28] H. Wang and D.-Y. Yeung, "A survey on Bayesian deep learning," *ACM Computing Surveys (CSUR)*, vol. 53, no. 5, pp. 1–37, 2020.
- [29] M. Zecchin, S. Park, O. Simeone, M. Kountouris, and D. Gesbert, "Robust Bayesian learning for reliable wireless AI: Framework and applications," *IEEE Trans. on Cogn. Commun. Netw.*, vol. 9, no. 4, pp. 897–912, 2023.
- [30] K. M. Cohen, S. Park, O. Simeone, and S. Shamai, "Bayesian active meta-learning for reliable and efficient AI-based demodulation," *IEEE Trans. Signal Process.*, vol. 70, pp. 5366–5380, 2022.
- [31] E. Nachmani, E. Marciano, L. Lugosch, W. J. Gross, D. Burshtein, and Y. Be'ery, "Deep learning methods for improved decoding of linear codes," *IEEE J. Sel. Topics Signal Process.*, vol. 12, no. 1, pp. 119–131, 2018.
- [32] E. Nachmani, Y. Be'ery, and D. Burshtein, "Learning to decode linear codes using deep learning," in *Annual Allerton Conference on Communication, Control, and Computing (Allerton)*, 2016.
- [33] W.-J. Choi, K.-W. Cheong, and J. M. Cioffi, "Iterative soft interference cancellation for multiple antenna systems," in *Proc. IEEE WCNC*, 2000.
- [34] J. Pearl, *Probabilistic reasoning in intelligent systems: networks of plausible inference*. Elsevier, 2014.
- [35] M. Tomlinson, C. J. Tjhai, M. A. Ambroze, M. Ahmed, and M. Jibril, *Error-Correction Coding and Decoding: Bounds, Codes, Decoders, Analysis and Applications*. Springer Nature, 2017.
- [36] Y. Gal and Z. Ghahramani, "Dropout as a Bayesian approximation: Representing model uncertainty in deep learning," in *International Conference on Machine Learning*. PMLR, 2016, pp. 1050–1059.
- [37] S. Buluki, R. Ardywibowo, S. Z. Dadaneh, M. Zhou, and X. Qian, "Learnable Bernoulli dropout for Bayesian deep learning," in *International Conference on Artificial Intelligence and Statistics*. PMLR, 2020, pp. 3905–3916.
- [38] L. Liu, C. Oestges, J. Poutanen, K. Haneda, P. Vainikainen, F. Quitin, F. Tufvesson, and P. De Doncker, "The COST 2100 MIMO channel model," *IEEE Wireless Commun.*, vol. 19, no. 6, pp. 92–99, 2012.
- [39] M. P. Naeini, G. Cooper, and M. Hauskrecht, "Obtaining well calibrated probabilities using bayesian binning," in *Proceedings of the AAAI Conference on Artificial Intelligence*, vol. 29, no. 1, 2015.
- [40] P. Becker, H. Pandya, G. Gebhardt, C. Zhao, C. J. Taylor, and G. Neumann, "Recurrent Kalman networks: Factorized inference in high-dimensional deep feature spaces," in *International Conference on Machine Learning*, 2019, pp. 544–552.
- [41] G. Revach, N. Shlezinger, X. Ni, A. L. Escoriza, R. J. Van Sloun, and Y. C. Eldar, "KalmanNet: Neural network aided Kalman filtering for partially known dynamics," *IEEE Trans. Signal Process.*, vol. 70, pp. 1532–1547, 2022.
- [42] D. H. Shmuel, J. P. Merkofer, G. Revach, R. J. van Sloun, and N. Shlezinger, "SubspaceNet: Deep learning-aided subspace methods for DoA estimation," *arXiv preprint arXiv:2306.02271*, 2023.
- [43] J. Knoblauch, J. Jewson, and T. Damoulas, "Generalized variational inference: Three arguments for deriving new posteriors," *arXiv preprint arXiv:1904.02063*, 2019.
- [44] A. Masegosa, "Learning under model misspecification: Applications to variational and ensemble methods," *Advances in Neural Information Processing Systems*, vol. 33, pp. 5479–5491, 2020.
- [45] W. R. Morningstar, A. Alemi, and J. V. Dillon, "Pacm-bayes: Narrowing the empirical risk gap in the misspecified bayesian regime," in *International Conference on Artificial Intelligence and Statistics*. PMLR, 2022, pp. 8270–8298.
- [46] V. Vovk, A. Gammerman, and G. Shafer, *Algorithmic learning in a random world*. Springer, 2005, vol. 29.
- [47] A. N. Angelopoulos and S. Bates, "A gentle introduction to conformal prediction and distribution-free uncertainty quantification," *arXiv preprint arXiv:2107.07511*, 2021.
- [48] K. M. Cohen, S. Park, O. Simeone, and S. Shamai, "Calibrating AI models for wireless communications via conformal prediction," *IEEE Trans. Mach. Learn. Commun. Netw.*, vol. 1, pp. 296–312, 2023.